Tethering RNA to chromatin for fluorescence microscopy based analysis of nuclear organization

Teresa Pankert, Thibaud Jegou [1], Maïwen Caudron-Herger [2], Karsten Rippe *

Research Group Genome Organization & Function, German Cancer Research Center (DKFZ) and Bioquant, Im Neuenheimer Feld 280, 69120 Heidelberg, Germany

ARTICLE INFO

ABSTRACT

Nuclear RNAs emerge as important factors to orchestrate the dynamic organization of the nucleus into functional subcompartments. By tethering RNAs to distinct genomic loci, RNA-dependent chromatin changes can be dissected by fluorescence microscopic analysis. Here we describe how this approach is implemented in mammalian cells. It involves two high-affinity protein-nucleic acid interactions that can be established with a number of different protein domains and DNA and RNA sequences. A prototypic system is described here in detail: It consists of the binding of MS2 bacteriophage coat protein to its RNA recognition sequence and the interaction between the bacterial LacI repressor protein to its target *lac*O operator DNA sequence. Via these interactions RNAs tagged with the MS2 recognition sequences can be recruited to a locus with integrated *lac*O repeats. By inducing RNA-chromatin binding a number of RNA-dependent activities can be dissected: (i) The RNA-induced compaction or decondensation of chromatin, (ii) identification of RNA-interacting chromatin modifiers that set epigenetic signals such as post-translational histone modifications, and (iii) nuclear relocation of a genomic locus targeted by the tethered RNA. Thus, a variety of RNA-dependent activities can be evaluated with the MS2-LacI system, which are crucial for understanding how RNA shapes nuclear organization.

1. Introduction

RNA production is regulated via the composition and spatial organization of chromatin and its nuclear environment. At the same time the proteins encoded by these RNAs as well as RNA transcripts themselves feed back on nuclear organization and genome function [1–4]. As such, they play important roles for the organization of nuclear subcompartments [5,6], for chromatin state changes [7–11], and for regulating gene expression [1,3,12,13]. A wide range of mechanisms has been proposed on how nuclear RNAs exert these activities [14]: RNAs might act as (i) a scaffold for higher order chromatin organizing ribonucleoprotein complexes [15–21], (ii) targeting factors of chromatin modifying complexes to genomic loci and to regulate their enzymatic activities [22–24], (iii) decoys that titrate away DNA-binding proteins [25,26], (iv) architectural factors mediating chromatin folding [12], or (v) nucleation sites for the biogenesis of various nuclear bodies [27–31].

In order to functionally characterize nuclear RNAs in single living cells as well as *in situ* after fixation, fluorescence microscopy based approaches are the method of choice. The sequence specific tagging and fluorescent labeling of RNA can be accomplished by engineering a high affinity protein binding sequence in one or more copies into the RNA of interest. A frequently applied pair of RNA sequence and RNA-binding protein is the bacteriophage MS2 stem loop sequence fused to an RNA of interest (MS2-RNA), which is recognized and bound by the MS2 bacteriophage coat protein (MS2-BCP) [6,32]. This system has extensively been exploited for investigating RNA in living cells [33–41]. In addition to MS2-BCP other high affinity RNA-binding proteins can be used together with their corresponding RNA recognition sequences, which might offer advantages for specific applications [42,43]. These include the bacteriophage lambda *N* protein [34,44,45], the Tat (trans-activator) peptide from the bovine immunodeficiency virus [46] or the bacteriophage PP7 coat protein [47,48].

To recruit the MS2-RNA to a specific chromatin locus and to examine its effect on the local chromatin environment a second high affinity interaction is exploited. It typically involves a stable integration of bacterial operator repeats into the genome, to which a bacterial repressor binds with high affinity. In the present work, we focus on the combination of *E. coli lac* repressor (LacI) binding to its *lac*O operator sequence [49,50]. Equivalent pairs that allow

---

tagging of genomic loci are *tet* repressor (TetR) and *tet*O operator sequences [51], LexA protein binding to the *lex*A sequence [52,53] as well as ParB protein together with the *par*S recognition sequence [54–56]. By tagging the repressor proteins with fluorescent proteins such as GFP, these experimental systems have been used for a variety of studies. The previous work for example addressed the movements of chromatin loci in living cells [57–60], the decondensation and acetylation of chromatin after recruitment of the transcriptional activator VP16 [61], the condensation and methylation of chromatin after recruitment of heterochromatin protein 1 (HP1) [62], the dynamics of gene expression [38], and protein-protein interactions in the nuclei of mammalian cells by recruiting proteins of interest to chromatin [63,64].

Here, we describe the use of the LacI-*lac*O system to recruit MS2-RNAs to chromatin. The methods can be easily adapted to the alternative RNA-binding proteins/RNA sequences (lambda *N* protein, Tat peptide, PP7) and genomic targeting interactions (TetR-*tet*O, LexA-*lex*A, ParB-*par*S) mentioned above. In a corresponding manner, endogenous loci can be tagged with transcription activator-like effector (TALE)-based strategies [65,66] or the CRISPR/dCas9 system with an endonuclease-deficient Cas9 protein [67,68]. For experimental data acquisition the experiments described here use imaging by confocal fluorescence laser scanning microscopy (CLSM) as readout. However, it is noted that the method of MS2 tagging of RNA is compatible with a variety of fluorescence imaging modalities [69]. It is applicable to studies of various activities, by which RNA affects chromatin and nuclear organization. These comprise RNA-mediated changes of chromatin compaction, chromatin composition and modification as well as the sub-nuclear localization of a genomic locus. Thus, the approach is remarkably versatile to dissect the role of RNA for nuclear organization by fluorescence microscopy based methods of in living or fixed cells.

2. Overview of the method

2.1. The MS2-LacI recruitment system

Naturally, the *lac*O sequence is part of the *E. coli lac* operon that regulates the bacterial lactose transport and metabolism. The *lac*O DNA sequence is bound by LacI repressor protein with high affinity and specificity even when this sequence is part of an *in vitro* reconstituted nucleosome without displacing the histone octamer [70,71]. Because of its particularly high specific binding affinity the combination of LacI repressor and *lac*O binding sites can be exploited to recruit defined proteins to chromatin by coupling them to LacI [72–74]. Repeats of *lac*O sequences are stably integrated into eukaryotic genomes to provide an array of chromosomal binding sites for the LacI fusion protein [59,73,74] (Fig. 1A). The three cell lines used in the methods and experiments described here (EC4, F4 2B8, AO3) have a single integration site of the *lac*O repeat array. Transfecting these cells with LacI fused to a fluorescent protein allows tracing the integrated *lac*O locus by fluorescence microscopy. To tether RNA to the *lac*O arrays, the MS2-BCP is fused with GFP and LacI to yield the MS2-BCP-GFP-LacI construct (Fig. 1A). The RNA of interest is tagged with several MS2 stem loop sequences to enhance the interactions. In the experiments described here constructs with 18 MS2 loops were used. Since repetitive sequences are prone to loss during plasmid amplification this needs to be accounted for by selecting appropriate *E. coli* strains (see protocol in Section 3.2). MS2-BCP binds as a dimer to the MS2-loops with high affinity [32] and a MS2-BCP dimer fusion sequence can be used to create preformed MS2-BCP dimers [75]. Via binding of MS2-BCP-GFP-LacI at the *lac*O array the interacting MS2-RNA is enriched at this locus and its influence on the chro-

matin environment is studied. The applications of the MS2-LacI system described here include the following assays: (i) RNA induced chromatin compaction (Fig. 1B). As described previously, RNA is a crucial factor to control the chromatin compaction state [4,7]. (ii) Analysis of RNA-dependent chromatin protein content and epigenetic signals as for example histone modifications. The interacting proteins can be detected in fluorescence two-color experiments with a given RNA-binding protein (RBP) fused for example to red fluorescent protein (RFP) or via immunofluorescence against a protein or its post-translational modifications (Fig. 1C). (iii) Sub-nuclear localization changes upon RNA tethering of a genomic locus (Fig. 1D). An example for this type of activity is the repositionig of the *lac*O array in relation to nucleoli that has been described recently [11].

2.2. Generation of cell lines with stably integrated lacO arrays

Several laboratories have generated mammalian cell lines with stable integrations of *lac*O and/or *tet*O operator sequence arrays. A non-comprehensive overview of these cell lines is given in Table 1. Protocols for the construction of these cell lines are given in the respective publications and published protocols [52,76] and in Section 3.1 below. They are based on the following strategy: Plasmids carrying arrays of the specific sequences and a selection marker are integrated into the genomes of the target cell lines. The cell lines can be distinct with respect to the chromosomal integration loci, the integration sizes and the number of integration sites per cell (Fig. 2, Table 1). The number of integrations can be determined using Southern hybridization of genomic DNA after restriction enzyme digestion using a restriction site that is unique in the vector carrying the *lac*O sequence. Fluorescent *in situ* hybridization (FISH) of metaphase chromosomes serves to identify the localization of the integration [38,57,60,62,77,78]. The insertion loci can be visualized in stable clones by transiently transfecting the cells with a construct coding for the LacI fused to GFP or mRFP. In the experiments with human cell lines described here, the U2OS cell lines EC4 (Fig. 2B, *lac*O repeat next to a telomere at chromosome 3p) and F4 2B8 (Fig. 2D, *lac*O repeat next to a centromere at chromosome 2q) were used. In addition, another single integration clone (FB4, Fig. 2A), a cell line with three chromosomes with *lac*O integration (F6B2, Fig. 2E) and one with a combination of *lac*O and *tet*O tagged chromosomes (BiC3, Fig. 2F) are depicted. The *lac*O integrations were generated using the plasmid pLAU43 containing 240 copies of the *lac* operator [79] as described in the detailed protocol 3.1 below. To identify the precise genomic location of the integrated *lac*O arrays, multicolor FISH to identify the chromosomes and FISH against the *lac*O sequences was applied. The third *lac*O array-containing cell line used here was the AO3 cell line, which was generated by Belmont and co-workers [73,74]. It is based on the DG44 CHO cell line with a deletion of the dihydrofolate reductase (DHFR) locus [80] transfected with the pSV2-DHFR-8.32 plasmid containing the *lac*O sequence. DHFR was used as a marker for selection of stable transformants.

2.3. Detecting RNA at the lacO array

In order to observe RNAs after recruitment to the *lac*O arrays, the RNA molecules need to be labeled. The fusion MS2-BCP with an auto-fluorescent domain (e.g. GFP, RFP) provides an RNA label (Fig. 1A) that has been also previously exploited for tracing RNA [33–37]. However, when evaluating an MS2-BCP-GFP-LacI construct enriched at a *lac*O repeat, it cannot be inferred to which extend the GFP-signal reflects RNA molecules bound to the MS2-BCP domain. Accordingly, an additional test needs to be conducted to assess the enrichment of RNA via the chromatin-tethering construct. To visualize RNA, a number of RNA aptamers have been
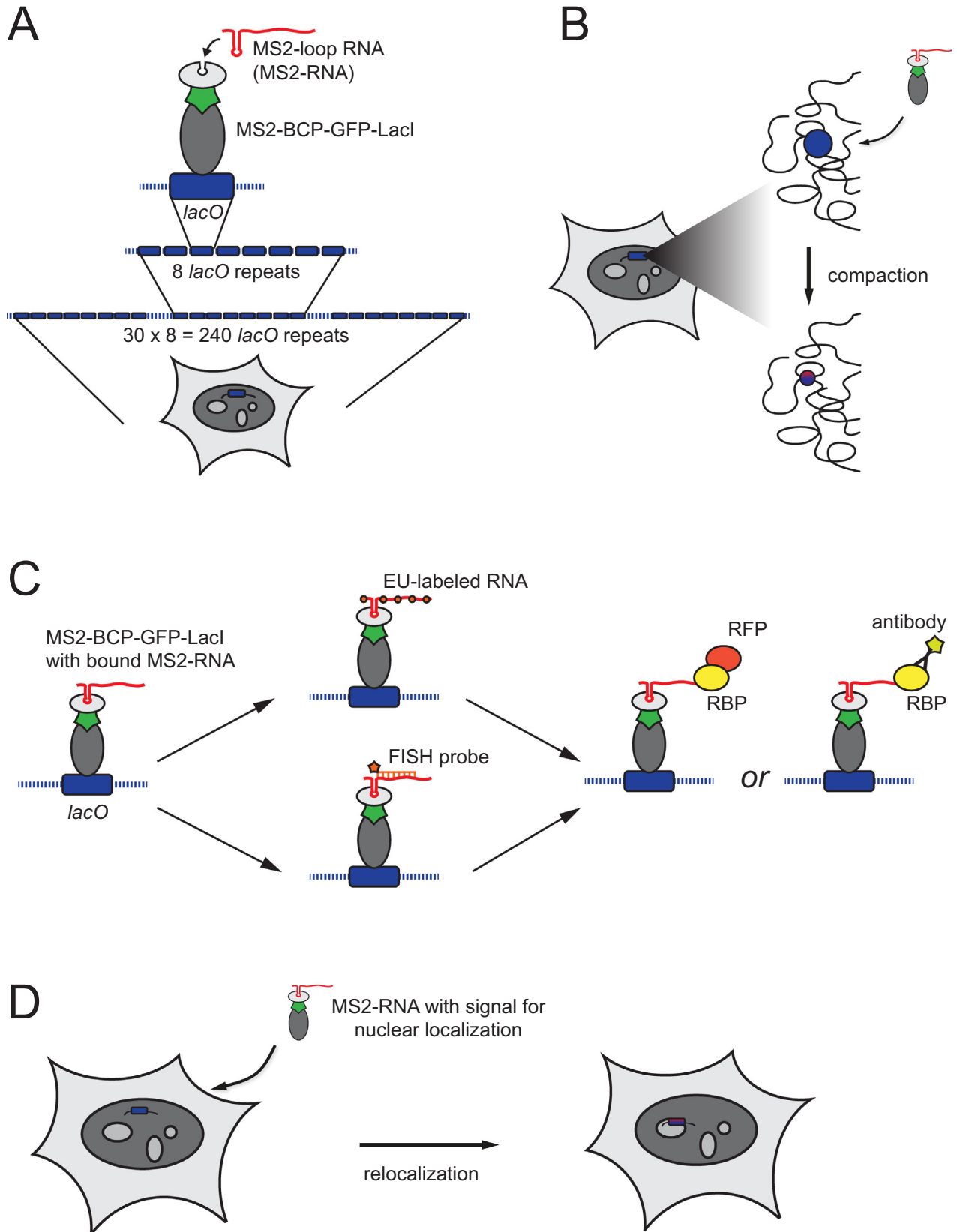
Fig. 1. Scheme of the MS2-LacI system and its applications. Different readouts of the function of an MS2 loop-containing RNA (MS2-RNA) of interest can be implemented to detect changes in chromatin organization. (A) Scheme of RNA recruitment approach. Arrays of the *lac*O repeats are stably integrated into the genome of mammalian cells. The MS2 stem loop-tagged RNA (MS2-RNA) binds to a protein fusion construct of MS2 bacteriophage coat protein (MS2-BCP) and fluorescent LacI repressor (GFP-LacI) referred to here as MS2-BCP-GFP-LacI. For simplicity only one of the MS2 stem loops sequences is shown although typically multiple copies are present. (B) RNA-induced chromatin compaction. (C) Analysis of MS2-RNA dependent chromatin protein content and modifications. The recruited RNA transcript can be visualized by EU incorporation or by RNA-FISH. Interacting proteins can be detected in fluorescence two-color experiments: either by a fusion of the RNA-binding protein with a red-fluorescent protein (RBP-RFP) or via immunofluorescence against a protein of interest. (D) Sub-nuclear localization changes upon RNA tethering, e.g. re-localization to nucleoli.

Table 1
Mammalian cell lines with *lac*O and/or *tet*O array integrations.

Clone	Insertion	Chromosomal location	Parent cell line	Species	References
U2OS 2-6-3	*lac*O, *tet*O, CMV promoter, MS2-RNA	n.d.	U2OS	Human	[38]
EC4	*lac*O	3p, Telomere	U2OS (HTB-96)	Human	[59]
FB4	*lac*O	3p Telomere	U2OS (HTB-96)	Human	[114]
FC2	*lac*O	11q, Telomere	U2OS (HTB-96)	Human	[114]
F4 1B4	*lac*O	21p, Telomere	U2OS (HTB-96)	Human	[114]
F4 2B8	*lac*O	2q, Centromere	U2OS (HTB-96)	Human	[59]
F4 2C8	*lac*O	14p, Telomere	U2OS (HTB-96)	Human	[114]
F6B2	*lac*O	6q, 11q, 12q	U2OS (HTB-96)	Human	[63]
BiC3	*lac*O, *tet*O	*lac*O: 6q, 11q, 12q; *tet*O: n.d.	U2OS (HTB-96)	Human	[114]
N/A	*lac*O	13q22, 5p14, 3q26.2, 13p, or 1q11	HT-1080	Human	[57]
N/A	*lac*O	Chr. 7	HeLa	Human	[115]
N/A	*lac*O, *tet*O, CMV promoter, MS2-RNA	n.d.	C2C12 myoblasts	Mouse	[5]
NIH2/4	*lac*O, *tet*O, *ISce*I restriction site	n.d.	NIH 3T3	Mouse	[60]
AO3	*lac*O	n.d.	CHO DG44 cell line with DHFR double knockout	Hamster	[77]
RRE-B1	*lac*O	n.d.	CHO DG44 cell line with DHFR double knockout	Hamster	[62]

The table shows an incomplete overview of mammalian cell lines with integrated *lac*O and *tet*O arrays.

identified, which bind molecules that only fluoresce when in complex with the RNA [81,82]. Alternatively, stem-loop shaped antisense oligonucleotides, so-called molecular beacon probes, can be used. These have an internally quenched fluorophore, whose fluorescence is restored upon RNA hybridization to the probe. These methods and their derivatives, however, might be prone to inefficient delivery and low stability of the probes in some cellular systems [83].

For labeling of the MS2-RNA after recruitment to the *lac*O arrays and fixation of the cells, we typically apply two methods (Fig. 1C, Fig. 3). The first approach involves the incorporation of ethynyluridine (EU) into RNA for direct labeling (see protocol in Section 3.4). This compound can be added to the cell culture medium and is readily incorporated into all newly synthesized RNAs. After fixation of the cells, the transcripts with incorporated EU are made visible by attaching a fluorophore to the EU moiety using an azide-alkyne cycloaddition reaction referred to as 'click' reaction [84]. Detection of RNA at the arrays is based on the assumption that the enrichment at the arrays is strong enough to distinguish it from the nuclear background, where nascent RNAs are constantly being produced. An alternative, more specific, approach is RNA fluorescence *in situ* hybridization (RNA-FISH) directed against either the MS2 stem loop sequence [85] or directly against the sequence of the RNA of interest (Fig. 1C, see Section 3.5 for a detailed protocol). For our quantitative analysis, we favor RNA-FISH directed against the MS2-stem loop sequences to ensure that the *lac*O array not only carries the MS2-BCP-GFP-LacI but also the MS2-RNA.

2.4. RNA-dependent chromatin compaction

The chromatin condensation state [86] has often been linked to its biological activity [87,88]. While silenced heterochromatin is more condensed, open and loosely packaged chromatin is thought to be more accessible for the transcription machinery as discussed in Ref. [89]. Transcriptional activity, on the other hand, can be regulated by RNAs that recruit, activate or inhibit chromatin modifiers [14]. In a previous study, it was shown that the *lac*O arrays integrated in a mammalian genome can be subjected to higher order chromatin unfolding in response to tethering a DNA-binding protein involved in nucleotide excision repair after UV-induced DNA damage [78]. It was concluded that the size of the array correlates with the compaction state of chromatin. The MS2-LacI recruitment system could thus also be used to investigate the compaction state of the *lac*O arrays in dependence of the RNA that is tethered to them (Fig. 1B).

In our previous work we found that a nuclear RNA fraction enriched in long 3′-UTR sequences maintains higher order chro-

matin in an open configuration [7]. Furthermore, 3′-UTRs also appear to have nuclear functions in addition to regulating mRNA stability, localization and translation. A large number of 3′-UTRs in human, mouse and fly are expressed independently from their associated protein-coding sequences, to which they are normally linked [90,91]. Furthermore, a systematic analysis of known long non-coding RNAs (lncRNAs) revealed similarities between 3′-UTRs and lncRNAs in terms of structural features and sequence composition [92]. To elucidate the nuclear activities of 3′-UTRs with respect to chromatin organization, the MS2-LacI-mediated recruitment system can be applied. This is demonstrated below in Section 4.2 and Fig. 4.

2.5. RNA-induced changes of chromatin content and epigenetic modifications

As discussed previously, chromatin is decorated with RNA. In addition, many chromatin-modifying enzymes bind to RNA, which could be essential for their targeting to specific genomic loci [4]. The MS2-LacI-mediated recruitment system is a well-suited system to study these aspects. It serves to recruit and immobilize specific RNAs on a defined chromatin locus in order to observe the subsequent enrichment of proteins at this locus. To readout the identity of these factors they can be overexpressed as a fusion protein with a fluorescent tag. Alternatively, one can perform immunofluorescent staining of protein candidates after fixing the cells (Fig. 1C). As an example, the Polycomb repressive complex 2 (PRC2) is investigated here with respect to RNA-dependent chromatin changes [93,94] (Section 4.3, Fig. 5). PRC2 has been described to modulate chromatin compaction state when in complex with EZH2 (enhancer of zeste homolog 2) [95–97]. The latter enzyme trimethylates histone H3 on lysine 27 (H3K27me3) [98]. Both EZH2 and SUZ12 (suppressor of zeste 12 homolog), a component of PRC2, have been shown to bind RNA [20,99–104], which makes PRC2 interesting in the context of investigating RNA mediated changes on chromatin with the MS2-LacI-mediated recruitment system. As an example for a PRC2-interacting RNA the RepA transcript is used, which has been extensively studied in the context of X chromosome inactivation in female mammalian cells. This 250 nucleotides long RNA originates from the first exon of the X inactivation specific transcript (XIST) and contains the so called A repeats, which form a very specific stem loop structure and are essential for XIST-mediated chromosome silencing [105,106]. The coordinated expression of this transcript regulates the recruitment of chromatin modifying factors that eventually render one of the X chromosomes in female mammalian cells inactive. The current model supports the view that PRC2 contacts RepA
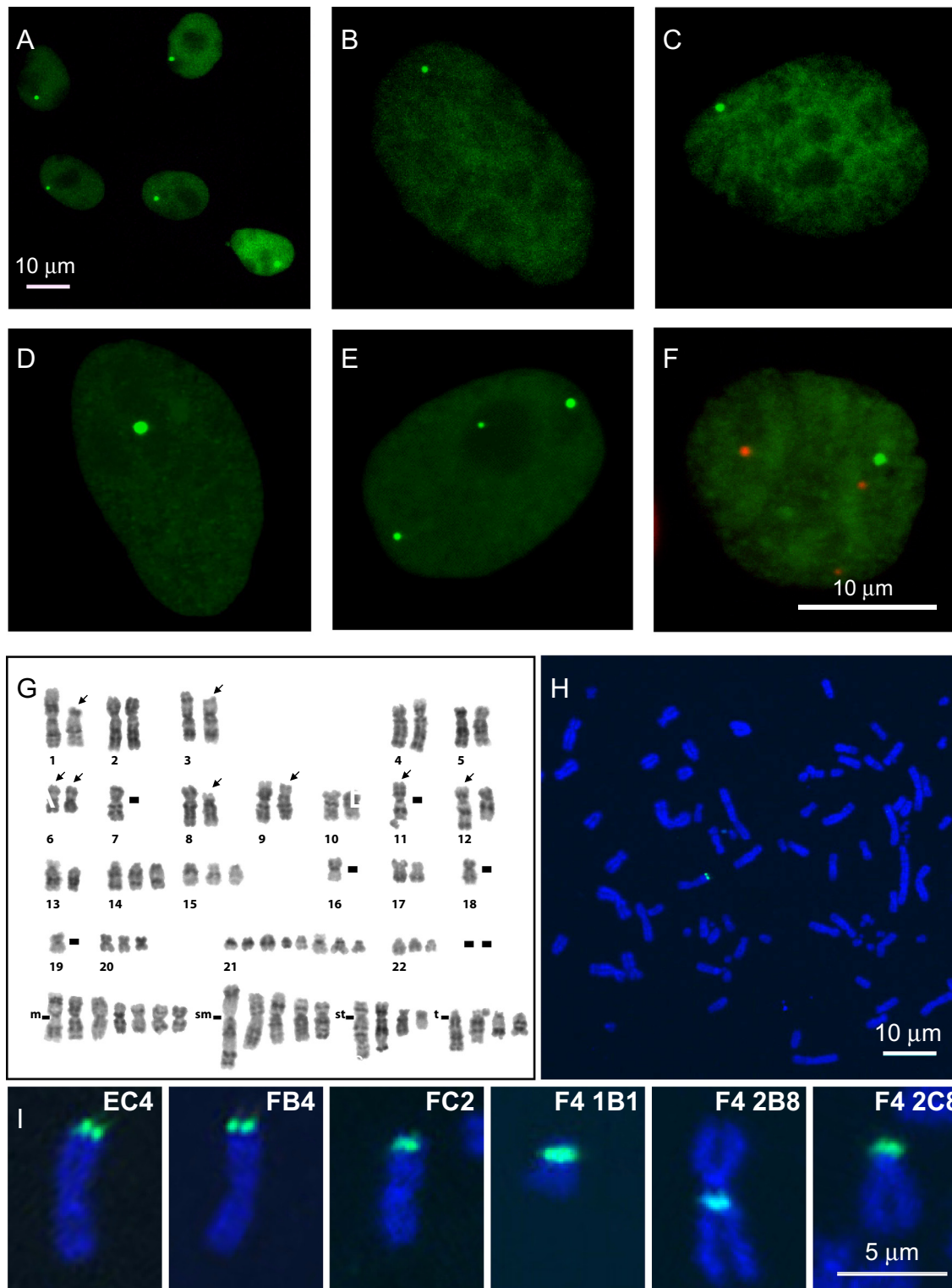
Fig. 2. Examples of generated clones with *lac*O and *tet*O arrays. The *lac*O and/or tetO arrays were stably integrated into the human U2OS cell line [59,114]. (A) FB4 transiently transfected with a LacI-GFP vector. (B) Same as panel A but for EC4 cell line. (C) Same as panel A but for FC2 cell line. (D) Same as panel A but for F4 2B8 cell line. (E) Same as panel A but for F6B2 cell line. (F) U2OS BiC3 cell line carrying *lac*O array and *tet*O array integrations. Cells were transiently co-transfected with LacI-RFP together with TetR-GFP. BiC3 was obtained by stably transfecting a *tet*O array vector in the F6B2 cell line. Thus, the three *lac*O inserts of the clone F6B2 are visible in BiC3 (in red) as well as a large *tet*O array insert (in green). (G) Identification of the *lac*O array integration chromosomal locus by FISH. Karyotyping of the U2OS cell line was done with the Giemsa banding technique. (H) The precise chromosomal integration of the arrays is determined by FISH on metaphase chromosomes using a fluorescently labeled probe coding for the *lac*O sequence. An example for the clone FB4 is given. (I) A typical set of metaphase chromosomes from different clones isolated with the stably integrated *lac*O array is shown.

via the EZH2 and SUZ12 subunits. This recruitment takes place co-transcriptionally and leads to PRC2 loading onto chromatin [107]. The MS2-LacI system provides a means of directly testing whether the RepA transcript can recruit EZH2 to chromatin in living cells (Section 4.3, Fig. 5). Furthermore it can be applied to investigate if a given RNA carries the activity to induce setting of the

A

| DNA | lacO array | EU-labeled RNA |

B

| DNA | lacO array | MS2 loop FISH |

− RNase A

+ RNase A
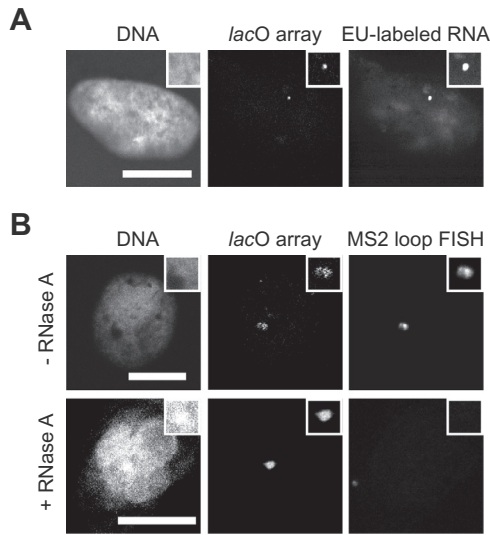
Fig. 3. Visualization of MS2 stem loop-tagged RNA recruited to lacO arrays with the MS2-BCP-GFP-LacI fusion protein. Cells were transfected with the MS2-BCP-GFP-LacI construct and a plasmid encoding for an MS2 stem loop-tagged RNA oligonucleotide of 60 nucleotides. (A) EC4 cells were treated with 1 mM EU overnight and EU was marked with a fluorophore using "click" chemistry after fixation. (B) AO3 cells were fixed 24 h after transfection and RNA-FISH with an ATTO-565-labeled probe directed against the MS2 stem loop sequence was performed. RNase A-treated cells were included in order to rule out unspecific binding of the RNA probe to DNA sequences. Insets show enlargements of the lacO arrays. Scale bars: 10 μm.

H3K27me3 modification at the lacO array (Section 4.4, Fig. 6). Similar to investigating the protein content of chromatin at the arrays, immunofluorescent staining is used to detect changes in the post-translational changes of the histones at the lacO arrays.

2.6. RNA-targeted sub-nuclear relocalization of genomic loci

The nucleus of mammalian cells is a heterogeneous environment with RNA as an important factor for nuclear architecture [4]. As described previously, specific RNA transcripts can trigger the nucleation of certain nuclear bodies [27–31]. Another important determinant of chromatin function is the localization of a given locus relative to other nuclear subcompartments. Interestingly, in a recent study we observed that the recruitment of Alu element-containing RNA transcripts increased the proportion of lacO arrays that were localized to the nucleolus [11], a nuclear organelle that can adapt its structure and transcriptional activity to the needs of the cell. Thus, the MS2-LacI-mediated recruitment system can also be applied to visualize RNA-dependent changes in the sub-nuclear localization of the loci. This example will be explained in more details in the Experimental examples Section below (Fig. 1D, Section 4.5, Fig. 7).

3. Detailed protocols

3.1. Generation of cell lines with stably integrated lacO arrays

Cell lines with stably integrated lacO arrays were obtained by co-transfection with a plasmid containing 240 repeats of lac
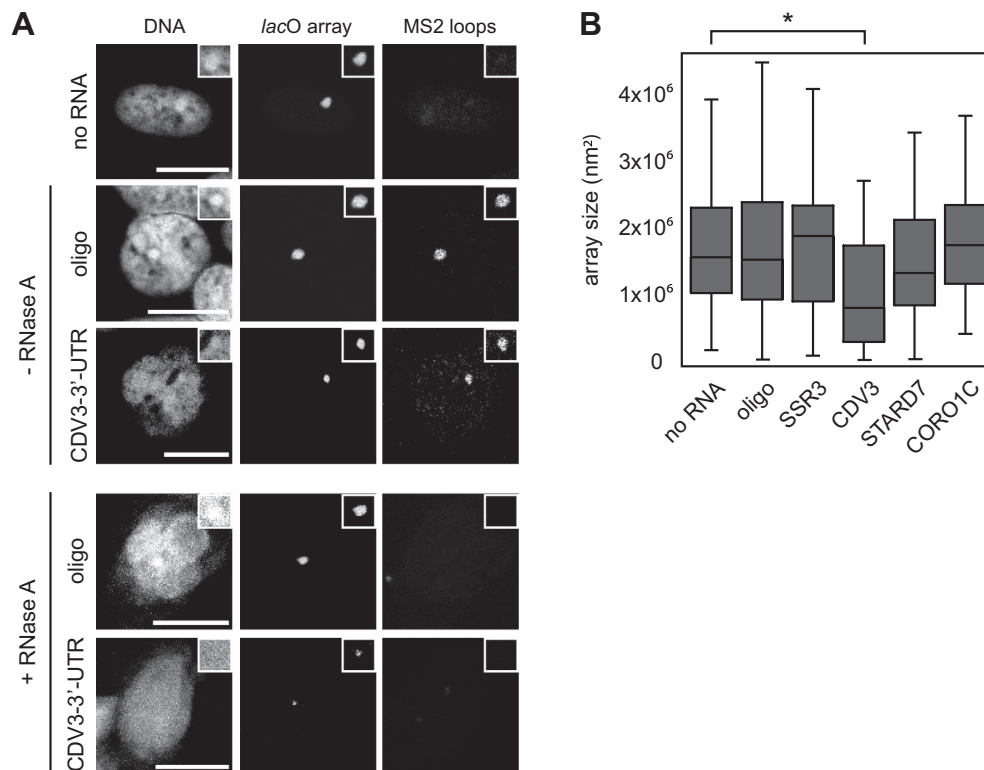
Fig. 4. RNA-dependent changes in chromatin compaction. AO3 cells containing a stable insertion of the bacterial lacO repeat sequence were transfected with a fusion protein of MS2-BCP-GFP-LacI and the RNA of interest tagged with the MS2 stem loop sequences. The MS2 loops were detected by RNA-FISH and nuclei were counterstained with DAPI. (A) CLSM images of cells transfected with no RNA, the MS2 stem loops with a 60 nucleotide-long oligonucleotide ("oligo") or the 3′-UTR of CDV3 tagged with the MS2 stem loops. Each RNA was transfected twice and one sample of each was treated with RNase A (lower two panels). Insets show enlargements of the lacO arrays. Scale bars: 10 μm. (B) Quantitative analysis of the size of the lacO array depending on the RNA recruited to it. The MS2 stem loop tagged oligonucleotide and the 3′UTRs of CDV3, SSR3, STARTD7, and CORO1C were transfected. The median, the upper and lower quartiles and the 95% confidence intervals are shown. $n > 50$, $^*p < 0.05$ (Wilcoxon test).

A

B
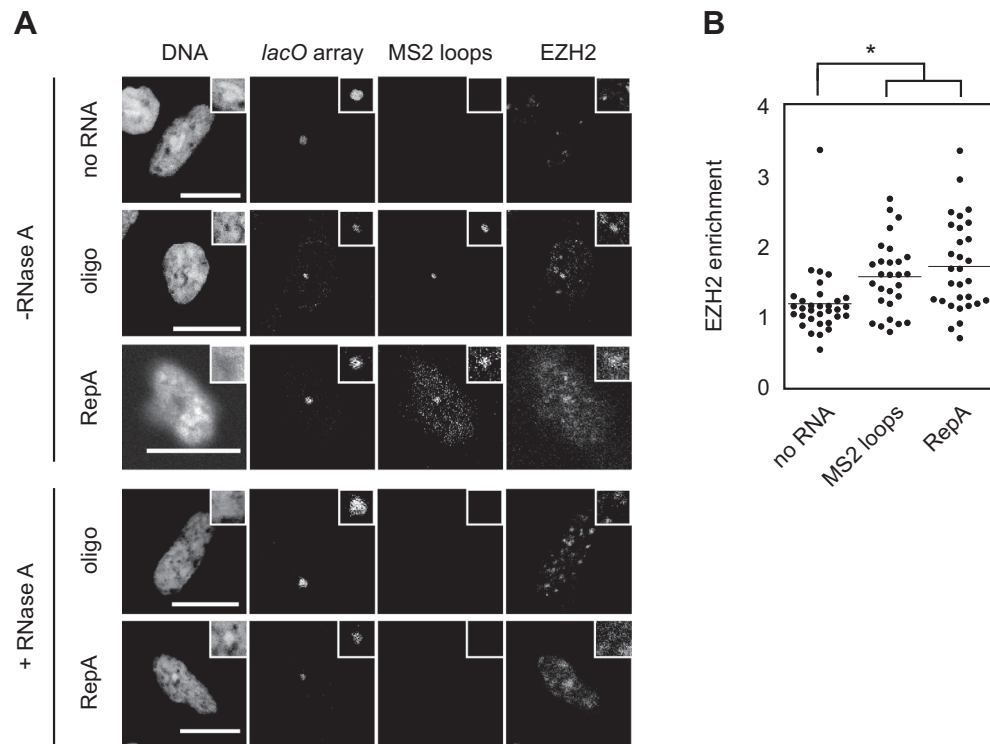
Fig. 5. RNA-dependent chromatin protein content. AO3 cells containing a stable insertion of the bacterial *lac*O repeat sequence were transfected with the MS2-BCP-GFP-LacI fusion protein and the RNA of interest tagged with the MS2 stem loop sequences. The MS2 loops were detected by RNA-FISH and EZH2 by immunostaining. (A) Nuclei were counterstained with DAPI. CLSM images of cells transfected with no RNA, the MS2 stem loops with a 60 nucleotide-long oligonucleotide ("oligo") or RepA tagged with the MS2 stem loops. Each RNA was transfected twice and one sample of each was treated with RNase A (lower panel). Insets show enlargements of the *lac*O arrays. Scale bar: 10 µm. (B) Quantitative analysis of the enrichment of EZH2 at the array as compared to the background, based on the fluorescent intensity of the EZH2 signal. $n > 30$, $^*p < 0.05$ (Wilcoxon test).

A

B
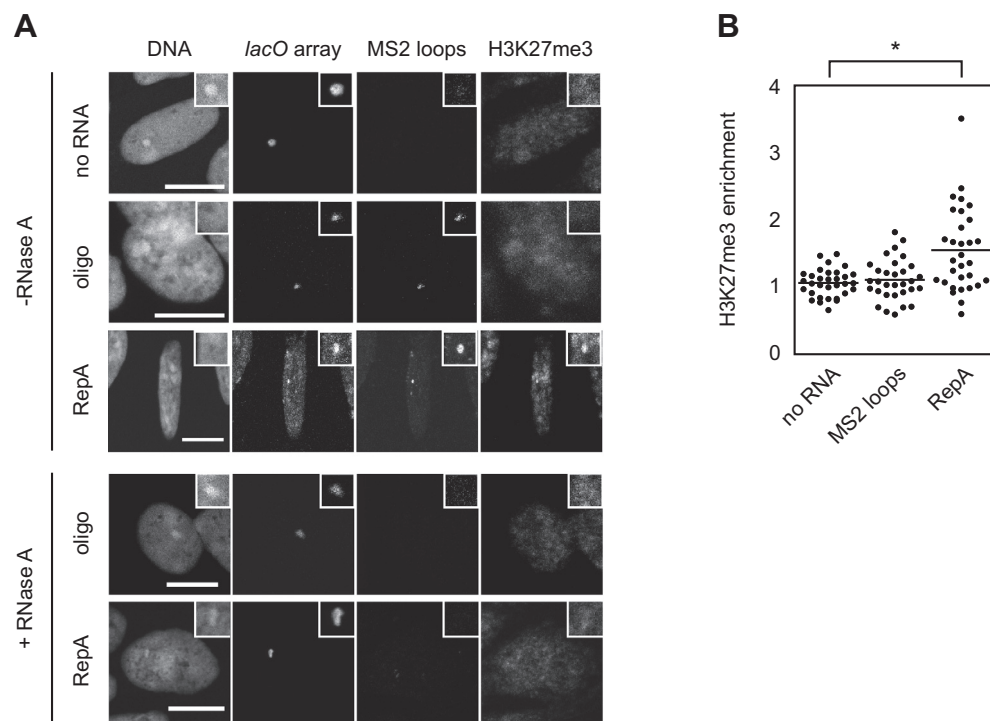
Fig. 6. RNA-dependent induction of the H3K27me3 histone modification. AO3 cells containing a stable insertion of the bacterial *lac*O repeat sequence were transfected with the MS2-BCP-GFP-LacI fusion protein and the RNA of interest tagged with the MS2 stem loop sequences. The MS2 loops were detected by RNA-FISH and H3K27me3 was visualized by immunostaining. Nuclei were counterstained with DAPI. (A) CLSM images of cells transfected with no RNA, the MS2 stem loops with a 60 nucleotide-long oligonucleotide or RepA tagged with the MS2 stem loops. Each RNA was transfected twice and one sample of each was treated with RNase A (lower panel). Insets show enlargements of the *lac*O arrays. Scale bar: 10 µm. (B) Quantitative analysis of the enrichment of H3K27me3 at the array as compared to the background, based on the fluorescent intensity of the H3K27me3 signal. $n > 30$, $^*p < 0.05$ (Wilcoxon test).
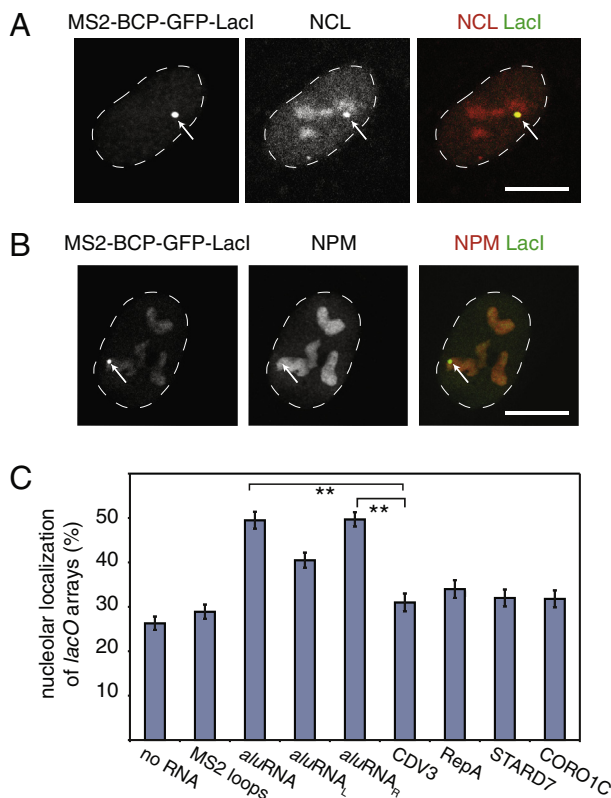
Fig. 7. RNA-dependent nuclear relocation of genomic loci. The *Alu* element-containing RNA transcripts promote nucleolar localization when tethered to the *lac*O locus in the U2OS F4 2B8 cell with a single stably integrated *lac*O array (figure adapted from Ref. [11]). (A) CLSM images of U2OS cells transfected with MS2-*alu*RNA$_R$ (right arm of the *alu*RNA). They reveal the localization of MS2-BCP-GFP-LacI (green in merged image) and NCL (immunofluorescence, red in the merged image). Note: the *alu*RNA induces the enrichment of NCL at the *lac*O locus. The arrow indicates the *lac*O array, which is associated with a nucleolar domain. Scale bars: 10 μm. (B) Same as in panel A but with NPM (immunofluorescence, red in the merged image). (C) MS2-loop-containing forward *alu*RNA, *alu*RNA$_L$ (left arm of the *alu*RNA), or *alu*RNA$_R$ were recruited to the *lac*O array. The propensity for nucleolar localization was evaluated as the average number of *lac*O arrays with tethered RNA detected in nucleoli (±95% CI) and is plotted in the bar chart. Calculations are based on analysis of more than 100 cells. $^{**}p < 0.01$, *t*-test, from the analysis of two independent biological replicates. As controls, no RNA, transcripts of the MS2 loop-containing RNA only and control MS2-tagged transcripts (*CDV3*, RepA, *STARD7* and *CORO1C*) were used.

operator sequence (pLAU 43, kindly provided by David Sherrat, Oxford) [108] together with a neomycin resistance coding vector (pcDNA3.1). Both vectors were linearized and mixed in a 1:5 or 1:10 ratio. U2OS cells growing in a 12-well plate were then transfected. After 24 h cells were trypsinized and transferred to a 12 cm tissue culture dish. 750 μg/ml G418 was added after 24 additional hours. The non-stably transfected cells died after 4–5 days and the complete selection procedure lasted for 10 days. During the selection phase, the medium was exchanged daily in order to remove the dead cells. About two to three weeks after beginning of the selection, single colonies were visible. The colonies were 1–1.5 mm in diameter and separated. 100–200 clones were picked with a 10 μl pipette tip and transferred to a 48-well plate. After one week, the surviving clones (30–50%) were trypsinized and transferred to two wells of a 24 well-plate. One of the plates, containing a glass coverslip in each well, was transiently transfected with LacI-GFP in order to screen the clones after fixation. The corresponding positive clones were grown from the other 24-well plate. Detailed protocols of how other laboratories generated cell lines can be found in a number of publications [38,52,57,60–62,73,74,76–78,108].

Cell culturing of *lac*O containing cell lines followed standard conditions. The EC4 and F4 2B8 U2OS cell lines were cultured in DMEM medium supplemented with 2 mM L-Glutamine, 10% FCS and 1% penicillin/streptomycin (v/v). The AO3 cells were grown in DMEM/F-12 medium supplemented with 2 mM fresh L-Glutamine, 20% FCS and 1% penicillin/streptomycin (v/v). All cells were grown at 37 °C in 5% CO$_2$.

3.2. Molecular cloning

All RNAs sequences were expressed from a pcDNA3.1 vector containing the MS2 stem loop sequences (pcDNA3.1-MS2) [109]. They were amplified by PCR using the Q5 polymerase and primers containing the *Not* I restriction site. Total HeLa cDNA was used as templates for PCR. PCR-products were purified using the Wizard SV Gel and PCR Clean-Up System (Promega, Germany). Restriction digestion of both insert and target vector were carried out using FastDigest enzymes (Thermo Fisher Scientific, USA). Phosphate residues of the vector were removed by Fast-AP phosphatase (Thermo Fisher Scientific, USA) for 30 min at 37 °C. Both inserts and vector fragments were purified by agarose gel extraction and ligated using the T4 DNA ligase (New England Biolabs). To amplify the ligated products, they were transformed into *E. coli* SURE 2 competent cells (Strategene, USA), which were grown in LB medium supplemented with ampicillin at a concentration of 100 μg/ml at 30 °C overnight. Rapid amplification of the pcDNA3.1-MS2 plasmid in *E. coli* strains like DH5α can lead to loss of some of the MS2 stem loop sequences. To maintain the full number of MS2 repeats, we recommend using the SURE 2 strain, which is recombination (*recB recJ*) deficient, and to grow them at 30 °C instead of 37 °C. Plasmids were then isolated using the nucleospin plasmid purification kit (Macherey Nagel, Germany) and verified by sequencing. All kits and enzymes were used according to the manufacturer's instructions. Plasmid amplification of pSV2-MS2-BCP-GFP-LacI [11] was carried out in DH5α competent bacteria in kanamycin (50 μg/ml) containing LB-ampicillin medium at 37 °C overnight and purified as described above.

3.3. Transient transfections

Transient transfection of plasmids into cells was conducted with Lipofectamine 2000 (Thermo Fisher Scientific, USA) according to the manufacturer's instructions. Briefly, cells were seeded 24 h prior to transfection to reach a confluence of 80–90% at the time point of transfection. The penicillin/streptomycin-containing medium was replaced by antibiotic-free medium. Plasmid DNA and lipofectamine were separately diluted in Opti-MEM (Thermo Fisher Scientific, USA) and were mixed, stirred rigorously and incubated at room-temperature for 20 min. Lipofectamine-DNA complexes were then added to the cells. The transfection mixes were removed from the cells 6–8 h after transfection and replaced with antibiotic-containing medium. Cells were fixed 24 h after transfection. Plasmids encoding the MS2 loop-containing RNAs and the plasmids encoding the MS2-GFP-LacI fusion protein were transfected at equal amounts. For microscopy cells were processed as described, but seeded on microscopy coverslips.

3.4. Ethynyl uridine labeling of RNA

To label RNAs with 5-ethynyl uridine (EU), cells were incubated with 1 mM EU overnight and fixed with 4% paraformaldehyde/PBS. EU-labeled transcripts were detected using Alexa Fluor 565 azide according to the Click-it RNA imaging Kit (Thermo Fisher Scientific, USA) and following the manufacturer instructions.

3.5. RNA fluorescence in situ hybridization

1. For RNA-FISH against the MS2 stem loops, cells were grown on coverslips and permeabilized in CSK buffer for 5 min on ice (100 mM NaCl, 300 mM sucrose, 3 mM MgCl$_2$, 10 mM PIPES pH 6.8, 0.5% Triton X 100) containing 10 mM vanadyl ribonucleoside complex (VRC, New England Biolabs, Germany) or 50 µg/ml RNase A (see notes below).
2. Cells were subsequently fixed with 4% paraformaldehyde/PBS for 15 min at room temperature.
3. Cells were dehydrated by sequential washes with ethanol (70%, 85%, and 100%) for 3 min each at room temperature and finally air-dried.
4. The slides were mounted upside down on a 5 µl drop of hybridization mix (see notes below) and sealed with rubber cement (Fixogum, Marabu) to avoid evaporation.
5. The probe was hybridized overnight in hybridization buffer at 37 °C in a humid hybridization chamber.
6. The next day, the slides were washed twice with 2X SSC, 50% formamide at room temperature for 15 min, once with 0.2X SSC, 0.1% Tween at 40 °C for 10 min and once with 2X SSC at room temperature for 5 min.
7. The slides were washed again in PBS for 5 min at room temperature.
8. Finally, the slides were incubate with 1× DAPI solution (Sigma-Aldrich, Germany) and washed again in PBS and water.
9. The slides were mounted and fixed in mowiol mounting medium (see notes below) on microscopy slides (Menzel-Gläser, Germany).

Notes:

- The RNase A control is needed to ensure that the RNA FISH probes hybridize to RNA and not to DNA with the same sequence.
- Preparation of the hybridization mix: Per slide, 50 ng of the 5′–Atto-565-labeled antisense probe that has been used in Ref. [85] with the sequence 5′–GTC GAC CTG CAG ACA TGG GTG ATC CTC ATG TTT TCT AGG CAA TTA–3′ was mixed with 10 µg salmon sperm DNA and 5 µl formamide. The mixture was heated to 37 °C for 10 min and 74 °C for 7 min before 5 µl hybridization buffer (30% dextran sulfate, 2 mg/mL BSA, 4× SSC) containing either 10 mM VRC or 50 µg/ml RNase A were added to the slides.
- Mowiol mounting medium preparation: 6 g of mowiol 4–88 (Sigma–Aldrich, USA), 6 g of glycerol and 6 mL of H$_2$O were mixed and stirred for 3–4 h at room temperature (the solution becomes highly viscous with time). 12 ml 0.2 M Tris-HCl pH 8.5 were added and the mixture was placed on a heating plate at 50 °C for 10 min with continuous stirring. After the mowiol dissolved, it was centrifuged at 5000g for 15 min. Aliquots were stored at −20 °C.

3.6. Immunofluorescence

For immunofluorescence in combination with RNA FISH, cells were processed as follows.

1. Cells were grown on coverslips and permeabilized in CSK buffer for 5 min on ice (100 mM NaCl, 300 mM sucrose, 3 mM MgCl$_2$, 10 mM PIPES pH 6.8, 0.5% Triton X-100) containing 10 mM vanadyl ribonucleoside complex (VRC, New England Biolabs, Germany) or 50 µg/ml RNase A (see notes above).
2. Cells were fixed with 4% paraformaldehyde/PBS for 15 min at room temperature.

3. The cells were then permeabilized for 5 min in ice-cold 0.5% Triton X-100/PBS (v/v).
4. Cells were washed three times for 5 min in PBS at room temperature.
5. They were blocked with 10% goat serum/PBS at room temperature for 30 min.
6. The slides were incubated for at least 1 h at room temperature with the first antibody (see notes below).
7. To remove excessive primary antibody, cells were washed three times 5 min with 0.02% NP40/PBS (v/v) at room temperature.
8. The secondary antibody was incubated at room temperature for 30 min.
9. Slides were washed three times 5 min in PBS at room temperature.
10. If further processed for RNA FISH, the slides were again fixed in 4% paraformaldehyde/PBS for 15 minutes at room temperature. The RNA-FISH protocol was conducted as described above.

Notes:

- Primary antibodies specific to the protein of interest (EZH2: Active Motif, #39875, H3K27me3: Active Motif, #39535, nucleolin (NCL): Santa Cruz Biotechnology, #sc-13057, nucleophosmin (NPM): Santa Cruz Biotechnology, #sc-56622) were diluted in the blocking solution.
- Appropriate secondary antibodies conjugated with fluorescent dyes were also diluted in the blocking solution (goat anti-mouse IgG (H + L) secondary antibody, Alexa Fluor 633 conjugate, Thermo Fisher Scientific, A-21052 and goat anti-rabbit IgG (H + L) secondary antibody, Alexa Fluor 633 conjugate, Thermo Fisher Scientific, A-21070).

3.7. Fluorescence microscopy

Confocal imaging was done with a Leica TCS SP5 confocal laser-scanning microscope equipped with a HCX PL APO lambda blue 63×/1.4 NA oil immersion objective (Leica Microsystems CMS GmbH, Mannheim, Germany). A near UV diode, diode-pumped solid-state, argon and helium-neon lasers were used for DAPI ($\lambda = 405$ nm), Alexa 488 or GFP ($\lambda = 488$ nm), Alexa 568 ($\lambda = 561$ nm) or Atto-565 and Alexa 633 ($\lambda = 633$ nm) excitation. For multi-color analysis sequential image acquisition was applied. The emission detection ranges were adjusted to minimize crosstalk between the different channels. The detection pinhole had a diameter corresponding to one airy disk.

3.8. Image analysis

ImageJ [110] was used for the analysis of microscopy pictures from single images or the maximum intensity projections of image stacks. For measurement of the particles size, images were segmented via thresholding and the function "Analyze Particles" was used to automatically determine the size of the *lac*O arrays. To measure protein enrichment at the *lac*O arrays, the fluorescent signal of the MS2-BCP-GFP-LacI protein was first used to identify the position of the arrays. The mean intensity values of the immunofluorescent staining against each protein of interest were then evaluated and the enrichment over the background signal in the nucleus of the same cell was calculated. In both cases only cells that showed a positive signal for the MS2-stem loops RNA-FISH at the arrays were taken into consideration.

To determine the relative position of the *lac*O arrays and the nucleolus compartment, both were fluorescently labeled and their signals were overlaid in ImageJ to analyze co-localization. The *lac*O

arrays were localized via the fluorescence signal of GBP-LacI-RFP. The nucleoli were localized by immunofluorescence of a nucleolar marker such as nucleophosmin (NPM) or nucleolin (NCL) (the first specific antibody was labeled via a secondary antibody conjugated to Alexa 633, Thermo Fisher Scientific).

4. Experimental examples

4.1. RNA can be detected at lacO arrays using EU incorporation or RNA-FISH

Labeling the RNA enriched at the array proved to be essential in all experiments conducted with MS2-LacI system to ensure that not only the MS2-BCP-GFP-LacI fusion protein but also the RNA of interest was enriched. To test different methods of RNA labeling at the lacO arrays, EC4 cells were transfected with the MS2-BCP-GFP-LacI fusion protein and a plasmid encoding for an MS2 stem loop-tagged RNA oligonucleotide of 60 nucleotides in length. At 6 h after transfection, EU was added to the medium of the transfected cells at a concentration of 1 mM and was allowed to be incorporated into newly synthesized RNAs overnight. At 24 h after transfection the cells were fixed and incorporated EU was stained using 'click' chemistry. Fig. 3A shows a cell, in which a clear enrichment of the EU signal could be seen at the arrays, visualized by the GFP-tagged LacI protein. In this experimental setup, EU is incorporated into all newly synthesized RNAs. Thus, although unlikely, the signal from the EU labeled RNA at the array might not originate solely from the MS2 stem loop-tagged RNA. Therefore, while incorporation of EU is easy to do and can be readily combined with immunofluorescence, it is less specific than directly detecting the MS2 stem loops-tagged RNA. Nonetheless, the enrichment of the RNA at the array was strong enough to identify the array via its EU-signal in comparison to the nuclear background signal. EU incorporation and labeling by "click" chemistry is thus a suited method to assess whether RNA is enriched at the lacO array when recruiting it there via the MS2-LacI-mediated recruitment system.

The second method involves RNA fluorescence *in situ* hybridization (RNA-FISH) with specific probes directed against the MS2 stem loop sequence. AO3 cells were transfected with the MS2-BCP-GFP-LacI fusion protein and the same plasmid encoding for a short MS2 stem loop-tagged RNA as above. Cells were fixed 24 h after transfection and RNA-FISH with a fluorescently labeled probe directed against the MS2 stem loop sequence was performed [85]. Alternatively, one could also make use of RNA-FISH probes directed directly against the sequence part that is specific for the RNA of interest. However, using probes against the MS2 stem loops is more versatile as the same probes can be applied for all RNAs of interest. Furthermore, the RNA is tagged with multiple MS2 stem loops, which provides an amplification of the fluorescent signal due to hybridization of several probes per transcript. Therefore, using RNA-FISH with probes directed against the MS2 stem loops was the method applied in all experiments described in the following. To ensure that the sequence detected by RNA-FISH is in fact the RNA sequence and not the DNA sequence of the plasmid, an RNase A-treated control was included in the analysis. Since RNase A cleaves all single stranded RNAs including the MS2 stem loop-tagged RNA, no RNA-FISH signal was expected after RNase A treatment. As depicted in Fig. 3B, an enrichment of the RNA-FISH signal that co-localizes with the MS2-BCP-GFP-LacI fusion protein could be seen (Fig. 3B, upper panel), whereas no RNA-FISH signal was detected at the array after RNase A treatment (Fig. 3B, bottom panel). Due to the high affinity of the MS2 stem loops for the MS2-BCP immobilized at the array, most of the MS2-tagged RNA was expected to be found at the array whereas very little should be distributed over the nucleus. Indeed, the background signal was very

low. Thus, RNA-FISH directed against the MS2 stem loop sequence is a well-suited method to detect enrichment of the MS2-RNA at genomic lacO sequences. This technique, however, requires some caution in the experimental handling as described in the detailed protocol provided in Section 3.5. Furthermore, due to incubation with formamide-containing buffers, this method is not compatible with every antibody used in subsequent immunofluorescent stainings. Additionally, controls that have been treated with RNase A have to be included to ensure that the probe only hybridized to the RNA and not the plasmid DNA.

4.2. Specific RNAs immobilized at the lacO array induce changes in chromatin compaction

To assess the ability of RNAs to change chromatin condensation AO3 cells containing a stable insertion of the bacterial lacO repeat sequence were transfected with a fusion protein of MS2-BCP-GFP-LacI and the RNA of interest tagged with 18 MS2 stem loop sequences. As exemplary RNA transcripts several 3'-UTRs were selected that were suggested to have putative chromatin organizing functions as described in a previous paper from our group [7]. For these experiments AO3 cells were used since the lacO array in this cell line is in a moderate condensation state. Accordingly, its decondensation [78] but also a further compaction can be observed. To detect RNA enrichment at the array, RNA–FISH with fluorescently labeled probes directed against the MS2 stem loop sequence was performed. The size of the arrays served as an indicator for the degree of chromatin compaction. Cells transfected with no RNA or with the MS2 stem loop sequence only were used as controls.

Fig. 4A shows representative CLSM images of cells that were transfected with no RNA, the MS2 stem loops attached to a short oligonucleotide of 60 nucleotide and the MS2-tagged 3'-UTR of CDV3 (carnitine deficiency-associated gene expressed in ventricle 3). The corresponding samples treated with RNase A (bottom panel) are also depicted demonstrating that the RNA-FISH only specifically hybridized to the MS2 RNA and not to the plasmid DNA. By visual inspection, it became clear that recruitment of the 3'-UTR of CDV3 decreased the size of the array. Recruiting just the MS2 loops did not affect the size of the array. This observation was substantiated by a quantitative analysis of the size of the arrays and comparison to other 3'-UTRs as displayed in Fig. 4B. Only the 3'-UTR of CDV3 but not those of SSR3 (signal sequence seceptor, gamma), STARD7 (star-related lipid transfer (START) domain containing 7) or CORO1C (coronin, actin binding protein, 1C) was able to significantly influence the degree of compaction of the lacO arrays locus.

4.3. RNAs immobilized at the lacO array recruit EZH2 with low specificity

Using the same experimental setup, we next examined whether RNAs immobilized at the array could also recruit specific protein interaction partners. As described above, EZH2 is a protein that has been described to bind RNAs of various nature both *in vitro* and *in vivo* [20,99–104,107]. Therefore it was used as an example for a protein that would be recruited to chromatin in an RNA-dependent manner. To do so, the same experimental setup as described above was used with an additional immunostaining directed against EZH2. The RepA transcript was tethered to the lacO array as an example of an RNA transcript that has previously been demonstrated to bind EZH2 [107]. As illustrated in Fig. 5A, all RNAs investigated in the MS2-LacI mediated chromatin recruitment system could enrich EZH2, even the MS2 stem loops with a short oligonucleotide attached to them. A quantitative analysis of the enrichment of EZH2 at the array was conducted (Fig. 5B) by

measuring the enrichment of EZH2 staining intensity over the background signal. This revealed an approximately 2-fold enrichment of EZH2 in an RNA-dependent manner.

With this assay, it remains unclear whether EZH2 is the component of the PRC2 complex that promotes the interaction with the RNAs. Alternatively, the interaction could also be mediated by one of the other PRC2 components that have RNA-binding capacities [107]. Nonetheless, this finding was in agreement with the previously reported promiscuous binding of RNA to the PRC2 complex observed both *in vitro* [111] and *in vivo* [20,99–104]. Thus, the MS2-LacI-mediated recruitment system is not only a well-suited system to study protein-protein interactions [6,63] but can also be used to study RNA-protein interactions in their cellular context.

4.4. Specific RNAs immobilized at the lacO array induce H3K27me3

The previous section shows that all RNAs tested induced an enrichment of EZH2 immobilized at the *lac*O array. Next, we investigated whether the MS2-LacI-mediated recruitment system could also be used to detect RNA-dependent changes on posttranslational histone modifications. Having seen that *lac*O-enriched RNAs can recruit EZH2 to the array, we investigated the presence of H3K27me3, which is set by EZH2. To do so, the same experimental setup as described above was used with an immunostaining directed against H3K27me3 instead of EZH2. Fig. 6 depicts that the RepA transcript not only recruited EZH2, but also led to an enrichment of the H3K27me3 mark at the array. However, the MS2 loop-tagged oligonucleotide did not. Interestingly, the H3K27me3 inducing activity was not observed to the same extent for the two RNAs tested, although they both recruited EZH2. The MS2-LacI-mediated recruitment system can thus be used to study the RNA-dependent activity of chromatin modifiers that set epigenetic marks like posttranslational histone modifications.

4.5. Specific RNAs immobilized at the lacO array induce their nucleolar relocalization

The approach of tethering RNA to *lac*O/*tet*O arrays can be also applied to evaluate the capacity of a given RNA sequence to mediate the targeting of a locus to a specific nuclear subcompartment (Fig. 1D). In the example shown here, the relative location of the fluorescently-tagged array was evaluated in the presence and absence of the MS2-RNA with respect to the nucleoli (Fig. 7). Here, the U2OS F4 2B8 cell line with a *lac*O array at a single genomic locus was used (Fig. 2D and I). First, we observed that the tethering of *Alu* element-containing RNA transcripts induced the recruitment of the nucleolar marker NCL (Fig. 7A) and NPM (Fig. 7B) to the arrays. Furthermore, it was observed that in the presence of the MS2-*alu*RNA at the array, the co-localization of the *lac*O array with nucleoli was significantly increased as compared to recruiting no RNA transcripts, an RNA containing only MS2 loops or other control RNA transcripts (Fig. 7 and Ref. [11]). Knowing that the *lac*O array is a megabase long element, its relocalization is an intriguing observation. It will be interesting to further decipher what type of interactions involving RNA transcripts and their protein-binding partners are driving such a rearrangement.

5. Concluding remarks

Here, we described several applications of the MS2-LacI system as an exemplary case for investigating nuclear organization and functions by tethering RNA to chromatin. While the microscopic readout was limited to CLSM imaging, the method is compatible with many other fluorescence microscopy-based techniques such as single particle tracking, light sheet microscopy, super-resolution microscopy, fluorescence correlation spectroscopy and fluorescence recovery after photobleaching. For genomic targeting, different interactions between bacterial high-affinity DNA-binding sites (LacI-*lac*O, TetR-*tet*O, LexA-*lex*A, ParB-*par*S) have been used. As described they all require the construction of dedicated cell lines where binding site repeats are stably integrated into the genome. To conduct corresponding experiments with endogenous sites, TALEs [65,66] or the CRISPR/dCas9 system [67,68] can be applied. However, in practice the need for sufficient fluorescent signal has restricted this type of application to studies of repetitive sequences like (peri)centromeres and telomeres. Interestingly, the CRISPR/dCas9 approach has also been adapted to recruit multiple RNA-binding proteins to an RNA scaffold that comprised binding sites for MS2-BPC or PP7 in 3′-extended guide RNA extended sequence [112]. Likewise, also the dCas9 protein can be fused to a repeating peptide array termed the SunTag to recruit up to 24 copies of the GFP [113]. Thus, new approaches are emerging to recruit specific RNA sequences to endogenous sites in conjunction with amplification of the fluorescence signal. In this manner, imaging of single protein molecules in living cells can be linked to tethering of an RNA of interest to chromatin to evaluate how RNAs affect genome functions on the single gene level.

References

[1] T.R. Mercer, J.S. Mattick, Understanding the regulatory and transcriptional complexity of the genome through structure, Genome Res. 23 (7) (2013) 1081–1088.
[2] P.J. Batista, H.Y. Chang, Long noncoding RNAs: cellular address codes in development and disease, Cell 152 (6) (2013) 1298–1307.
[3] J.H. Bergmann, D.L. Spector, Long non-coding RNAs: modulators of nuclear structure and function, Curr. Opin. Cell Biol. 26 (2014) 10–18.
[4] M. Caudron-Herger, K. Rippe, Nuclear architecture by RNA, Curr. Opin. Genet. Dev. 22 (2) (2012) 179–187.
[5] Y.S. Mao, H. Sunwoo, B. Zhang, D.L. Spector, Direct visualization of the co-transcriptional assembly of a nuclear body by noncoding RNAs, Nat. Cell Biol. 13 (1) (2011) 95–101.
[6] S.P. Shevtsov, M. Dundr, Nucleation of nuclear bodies by RNA, Nat. Cell Biol. 13 (2) (2011) 167–173.
[7] M. Caudron-Herger, K. Muller-Ott, J.P. Mallm, C. Marth, U. Schmidt, K. Fejes-Toth, K. Rippe, Coding RNAs with a non-coding function: maintenance of open chromatin structure, Nucleus 2 (5) (2011) 410–424.
[8] Z. Deng, J. Norseen, A. Wiedmer, H. Riethman, P.M. Lieberman, TERRA RNA binding to TRF2 facilitates heterochromatin formation and ORC recruitment at telomeres, Mol. Cell 35 (4) (2009) 403–413.
[9] L.H. Wong, K.H. Brettingham-Moore, L. Chan, J.M. Quach, M.A. Anderson, E.L. Northrop, R. Hannan, R. Saffery, M.L. Shaw, E. Williams, K.H. Choo, Centromere RNA is a key component for the assembly of nucleoproteins at the nucleolus and centromere, Genome Res. 17 (8) (2007) 1146–1160.
[10] L. Yang, C. Lin, W. Liu, J. Zhang, K.A. Ohgi, J.D. Grinstein, P.C. Dorrestein, M.G. Rosenfeld, NcRNA- and Pc2 methylation-dependent gene relocation between nuclear structures mediates gene activation programs, Cell 147 (4) (2011) 773–788.
[11] M. Caudron-Herger, T. Pankert, J. Seiler, A. Nemeth, R. Voit, I. Grummt, K. Rippe, Alu element-containing RNAs maintain nucleolar structure and function, EMBO J. 34 (2015) 2758–2771.
[12] H. Yao, K. Brick, Y. Evrard, T. Xiao, R.D. Camerini-Otero, G. Felsenfeld, Mediation of CTCF transcriptional insulation by DEAD-box RNA-binding protein p68 and steroid receptor RNA activator SRA, Genes Dev. 24 (22) (2010) 2543–2555.
[13] L. Yang, C. Lin, C. Jin, J.C. Yang, B. Tanasa, W. Li, D. Merkurjev, K.A. Ohgi, D. Meng, J. Zhang, C.P. Evans, M.G. Rosenfeld, LncRNA-dependent mechanisms of androgen-receptor-regulated gene activation programs, Nature 500 (7464) (2013) 598–602.
[14] J.L. Rinn, H.Y. Chang, Genome regulation by long noncoding RNAs, Annu. Rev. Biochem. 81 (2012) 145–166.
[15] T. Kino, D.E. Hurt, T. Ichijo, N. Nader, G.P. Chrousos, Noncoding RNA gas5 is a growth arrest- and starvation-associated repressor of the glucocorticoid receptor, Sci. Signal 3 (107) (2010) ra8.

[16] T. Hung, Y. Wang, M.F. Lin, A.K. Koegel, Y. Kotake, G.D. Grant, H.M. Horlings, N. Shah, C. Umbricht, P. Wang, Y. Wang, B. Kong, A. Langerød, A.-L. Børresen-Dale, S.K. Kim, M. van de Vijver, S. Sukumar, M.L. Whitfield, M. Kellis, Y. Xiong, D.J. Wong, H.Y. Chang, Extensive and coordinated transcription of noncoding RNAs within cell-cycle promoters, Nat. Genet. 43 (7) (2011) 621–629.

[17] Y. Kotake, T. Nakagawa, K. Kitagawa, S. Suzuki, N. Liu, M. Kitagawa, Y. Xiong, Long non-coding RNA ANRIL is required for the PRC2 recruitment to and silencing of p15(INK4B) tumor suppressor gene, Oncogene 30 (16) (2011) 1956–1962.

[18] K.L. Yap, S. Li, A.M. Munoz-Cabello, S. Raguz, L. Zeng, S. Mujtaba, J. Gil, M.J. Walsh, M.M. Zhou, Molecular interplay of the noncoding RNA ANRIL and methylated histone H3 lysine 27 by polycomb CBX7 in transcriptional silencing of INK4a, Mol. Cell 38 (5) (2010) 662–674.

[19] R.R. Pandey, T. Mondal, F. Mohammad, S. Enroth, L. Redrup, J. Komorowski, T. Nagano, D. Mancini-Dinardo, C. Kanduri, Kcnq1ot1 antisense noncoding RNA mediates lineage-specific transcriptional silencing through chromatin-level regulation, Mol. Cell 32 (2) (2008) 232–246.

[20] A.M. Khalil, M. Guttman, M. Huarte, M. Garber, A. Raj, D. Rivea Morales, K. Thomas, A. Presser, B.E. Bernstein, A. van Oudenaarden, A. Regev, E.S. Lander, J.L. Rinn, Many human large intergenic noncoding RNAs associate with chromatin-modifying complexes and affect gene expression, Proc. Natl. Acad. Sci. USA 106 (28) (2009) 11667–11672.

[21] M. Guttman, J. Donaghey, B.W. Carey, M. Garber, J.K. Grenier, G. Munson, G. Young, A.B. Lucas, R. Ach, L. Bruhn, X. Yang, I. Amit, A. Meissner, A. Regev, J.L. Rinn, D.E. Root, E.S. Lander, LincRNAs act in the circuitry controlling pluripotency and differentiation, Nature 477 (2011) 295–300.

[22] R.A. Gupta, N. Shah, K.C. Wang, J. Kim, H.M. Horlings, D.J. Wong, M.C. Tsai, T. Hung, P. Argani, J.L. Rinn, Y. Wang, P. Brzoska, B. Kong, R. Li, R.B. West, M.J. van de Vijver, S. Sukumar, H.Y. Chang, Long non-coding RNA HOTAIR reprograms chromatin state to promote cancer metastasis, Nature 464 (7291) (2010) 1071–1076.

[23] J.L. Rinn, M. Kertesz, J.K. Wang, S.L. Squazzo, X. Xu, S.A. Brugmann, L.H. Goodnough, J.A. Helms, P.J. Farnham, E. Segal, H.Y. Chang, Functional demarcation of active and silent chromatin domains in human HOX loci by noncoding RNAs, Cell 129 (7) (2007) 1311–1323.

[24] M. Huarte, M. Guttman, D. Feldser, M. Garber, M.J. Koziol, D. Kenzelmann-Broz, A.M. Khalil, O. Zuk, I. Amit, M. Rabani, L.D. Attardi, A. Regev, E.S. Lander, T. Jacks, J.L. Rinn, A large intergenic noncoding RNA induced by p53 mediates global gene repression in the p53 response, Cell 142 (3) (2010) 409–419.

[25] R.C. Spitale, M.C. Tsai, H.Y. Chang, RNA templating the epigenome: long noncoding RNAs as molecular scaffolds, Epigenetics 6 (5) (2011) 539–543.

[26] D.C. Zappulla, T.R. Cech, RNA as a flexible scaffold for proteins: yeast telomerase and beyond, Cold Spring Harb. Symp. Quant. Biol. 71 (2006) 217–224.

[27] M. Dundr, T. Misteli, Biogenesis of nuclear bodies, Cold Spring Harbor Perspect. Biol. 2 (12) (2010) a000711.

[28] M. Dundr, Seed and grow: a two-step model for nuclear body biogenesis, J. Cell Biol. 193 (4) (2011) 605–606.

[29] M. Dundr, Nuclear bodies: multifunctional companions of the genome, Curr. Opin. Cell Biol. 24 (3) (2012) 415–422.

[30] M. Dundr, Nucleation of Nuclear Bodies, Humana Press, Totowa, NJ, 2013, pp. 351–364.

[31] Y.S. Mao, B. Zhang, D.L. Spector, Biogenesis and function of nuclear bodies, Trends Genet. 27 (8) (2011) 295–306.

[32] H.E. Johansson, D. Dertinger, K.A. LeCuyer, L.S. Behlen, C.H. Greef, O.C. Uhlenbeck, A thermodynamic analysis of the sequence-specific binding of RNA by bacteriophage MS2 coat protein, Proc. Natl. Acad. Sci. USA 95 (16) (1998) 9244–9249.

[33] E. Bertrand, P. Chartrand, M. Schaefer, S.M. Shenoy, R.H. Singer, R.M. Long, Localization of ASH1 mRNA particles in living yeast, Mol. Cell 2 (4) (1998) 437–445.

[34] N. Daigle, J. Ellenberg, LambdaN-GFP: an RNA reporter system for live-cell imaging, Nat. Methods 4 (8) (2007) 633–636.

[35] T. Ozawa, Y. Natori, M. Sato, Y. Umezawa, Imaging dynamics of endogenous mitochondrial RNA in single living cells, Nat. Methods 4 (5) (2007) 413–419.

[36] M. Valencia-Burton, N.E. Broude, Visualization of RNA using fluorescence complementation triggered by aptamer-protein interactions (RFAP) in live bacterial cells, Curr. Protoc. Cell Biol. (2007) (Chapter 17, Unit 17 11).

[37] M. Valencia-Burton, R.M. McCullough, C.R. Cantor, N.E. Broude, RNA visualization in live bacterial cells using fluorescent protein complementation, Nat. Methods 4 (5) (2007) 421–427.

[38] S.M. Janicki, T. Tsukamoto, S.E. Salghetti, W.P. Tansey, R. Sachidanandam, K.V. Prasanth, T. Ried, Y. Shav-Tal, E. Bertrand, R.H. Singer, D.L. Spector, From silencing to gene expression: real-time analysis in single cells, Cell 116 (5) (2004) 683–698.

[39] X. Darzacq, J. Yao, D.R. Larson, S.Z. Causse, L. Bosanac, V. de Turris, V.M. Ruda, T. Lionnet, D. Zenklusen, B. Guglielmi, R. Tjian, R.H. Singer, Imaging transcription in living cells, Annu. Rev. Biophys. 38 (2009) 173–196.

[40] I.U. Rafalska-Metcalf, S.L. Powers, L.M. Joo, G. LeRoy, S.M. Janicki, Single cell analysis of transcriptional activation dynamics, PLoS ONE 5 (4) (2010) e10272.

[41] R.M. Martin, J. Rino, C. Carvalho, T. Kirchhausen, M. Carmo-Fonseca, Live-cell visualization of pre-mRNA splicing with single-molecule sensitivity, Cell Rep. 4 (6) (2013) 1144–1155.

[42] C. Keryer-Bibens, C. Barreau, H.B. Osborne, Tethering of proteins to RNAs by bacteriophage proteins, Biol. Cell 100 (2) (2008) 125–138.

[43] J. Coller, M. Wickens, Tethered function assays using 3′ untranslated regions, Methods 26 (2) (2002) 142–150.

[44] E. De Gregorio, T. Preiss, M.W. Hentze, Translation driven by an eIF4G core domain in vivo, EMBO J. 18 (17) (1999) 4865–4874.

[45] J. Baron-Benhamou, N.H. Gehring, A.E. Kulozik, M.W. Hentze, Using the lambdaN peptide to tether proteins to RNAs, Methods Mol. Biol. 257 (2004) 135–154.

[46] M. Wakiyama, Y. Kaitsu, R. Muramatsu, K. Takimoto, S. Yokoyama, Tethering of proteins to RNAs using the bovine immunodeficiency virus-Tat peptide and BIV-TAR RNA, Anal. Biochem. 427 (2) (2012) 130–132.

[47] F. Lim, D.S. Peabody, RNA recognition site of PP7 coat protein, Nucleic Acids Res. 30 (19) (2002) 4138–4144.

[48] F. Lim, T.P. Downey, D.S. Peabody, Translational repression and specific RNA binding by the coat protein of the Pseudomonas phage PP7, J. Biol. Chem. 276 (25) (2001) 22507–22513.

[49] A.S. Belmont, Visualizing chromosome dynamics with GFP, Trends Cell Biol. 11 (6) (2001) 250–257.

[50] C.H. Chuang, A.S. Belmont, Moving chromatin within the interphase nucleus-controlled transitions?, Semin Cell Dev. Biol. 18 (5) (2007) 698–706.

[51] J. Dworkin, R. Losick, Does RNA polymerase help drive chromosome segregation in bacteria?, Proc Natl. Acad. Sci. USA 99 (22) (2002) 14089–14094.

[52] I. Loïodice, M. Dubarry, A. Taddei, Scoring and Manipulating Gene Position and Dynamics Using FROS in Budding Yeast, John Wiley & Sons Inc., Hoboken, NJ, USA, 2001.

[53] J.C. Tang, J. Szikra, Y. Kozorovitskiy, M. Teixiera, B.L. Sabatini, B. Roska, C.L. Cepko, A nanobody-based system using fluorescent proteins as scaffolds for cell-specific gene manipulation, Cell 154 (4) (2013) 928–939.

[54] Z. Gitai, M. Thanbichler, L. Shapiro, The choreographed dynamics of bacterial chromosomes, Trends Microbiol. 13 (5) (2005) 221–228.

[55] Y. Li, K. Sergueev, S. Austin, The segregation of the Escherichia coli origin and terminus of replication, Mol. Microbiol. 46 (4) (2002) 985–996.

[56] H.J. Nielsen, J.R. Ottesen, B. Youngren, S.J. Austin, F.G. Hansen, The Escherichia coli chromosome is organized with the left and right chromosome arms in separate cell halves, Mol. Microbiol. 62 (2) (2006) 331–338.

[57] J.R. Chubb, S. Boyle, P. Perry, W.A. Bickmore, Chromatin motion is constrained by association with nuclear compartments in human cells, Curr. Biol. 12 (6) (2002) 439–445.

[58] W.F. Marshall, A. Straight, J.F. Marko, J. Swedlow, A. Dernburg, A. Belmont, A. W. Murray, D.A. Agard, J.W. Sedat, Interphase chromosomes undergo constrained diffusional motion in living cells, Curr. Biol. 7 (12) (1997) 930–939.

[59] T. Jegou, I. Chung, G. Heuvelman, M. Wachsmuth, S.M. Gorisch, K.M. Greulich-Bode, P. Boukamp, P. Lichter, K. Rippe, Dynamics of telomeres and promyelocytic leukemia nuclear bodies in a telomerase-negative human cell line, Mol. Biol. Cell 20 (7) (2009) 2070–2082.

[60] E. Soutoglou, J.F. Dorn, K. Sengupta, M. Jasin, A. Nussenzweig, T. Ried, G. Danuser, T. Misteli, Positional stability of single double-strand breaks in mammalian cells, Nat. Cell Biol. 9 (6) (2007) 675–682.

[61] T. Tumbar, A.S. Belmont, Interphase movements of a DNA chromosome region modulated by VP16 transcriptional activator, Nat. Cell Biol. 3 (2) (2001) 134–139.

[62] P.J. Verschure, I. van der Kraan, W. de Leeuw, J. van der Vlag, A.E. Carpenter, A. S. Belmont, R. van Driel, In vivo HP1 targeting causes large-scale chromatin condensation and enhanced histone lysine methylation, Mol. Cell. Biol. 25 (11) (2005) 4552–4564.

[63] I. Chung, H. Leonhardt, K. Rippe, De novo assembly of a PML nuclear subcompartment occurs through multiple pathways and induces telomere elongation, J. Cell Sci. 124 (Pt 21) (2011) 3603–3618.

[64] K. Zolghadr, O. Mortusewicz, U. Rothbauer, R. Kleinhans, H. Goehler, E.E. Wanker, M.C. Cardoso, H. Leonhardt, A fluorescent two-hybrid assay for direct visualization of protein interactions in living cells, Mol. Cell. Proteomics 7 (11) (2008) 2279–2287.

[65] Y. Miyanari, C. Ziegler-Birling, M.E. Torres-Padilla, Live visualization of chromatin dynamics with fluorescent TALEs, Nat. Struct. Mol. Biol. 20 (11) (2013) 1321–1324.

[66] H. Ma, P. Reyes-Gutierrez, T. Pederson, Visualization of repetitive DNA sequences in human chromosomes with transcription activator-like effectors, Proc. Natl. Acad. Sci. USA 110 (52) (2013) 21048–21053.

[67] B. Chen, L.A. Gilbert, B.A. Cimini, J. Schnitzbauer, W. Zhang, G.W. Li, J. Park, E. H. Blackburn, J.S. Weissman, L.S. Qi, B. Huang, Dynamic imaging of genomic loci in living human cells by an optimized CRISPR/Cas system, Cell 155 (7) (2013) 1479–1491.

[68] T. Anton, S. Bultmann, H. Leonhardt, Y. Markaki, Visualization of specific DNA sequences in living mouse embryonic stem cells with a programmable fluorescent CRISPR/Cas system, Nucleus 5 (2) (2014) 163–172.

[69] R.A. Coleman, Z. Liu, X. Darzacq, R. Tjian, R.H. Singer, T. Lionnet, Imaging transcription: past, present, and future, Cold Spring Harbor Symp. Quant. Biol. 80 (2015) 1–8.

[70] M.V. Chao, J.D. Gralla, H.G. Martinson, lac Operator nucleosomes. 1. Repressor binds specifically to operator within the nucleosome core, Biochemistry 19 (14) (1980) 3254–3260.

[71] M.V. Chao, H.G. Martinson, J.D. Gralla, lac Operator nucleosomes. 2. lac Nucleosomes can change conformation to strengthen binding by lac repressor, Biochemistry 19 (14) (1980) 3260–3269.

[72] M.C. Hu, N. Davidson, The inducible lac operator-repressor system is functional in mammalian cells, Cell 48 (4) (1987) 555–566.

[73] C.C. Robinett, A. Straight, G. Li, C. Willhelm, G. Sudlow, A. Murray, A.S. Belmont, In vivo localization of DNA sequences and visualization of large-scale chromatin organization using lac operator/repressor recognition, J. Cell Biol. 135 (6 Pt 2) (1996) 1685–1700.

[74] A.S. Belmont, A.F. Straight, In vivo visualization of chromosomes using lac operator-repressor binding, Trends Cell Biol. 8 (3) (1998) 121–124.

[75] D.S. Peabody, F. Lim, Complementation of RNA binding site mutations in MS2 coat protein heterodimers, Nucleic Acids Res. 24 (12) (1996) 2352–2359.

[76] Y.G. Strukov, A.S. Belmont, Development of Mammalian Cell Lines with lac Operator-Tagged Chromosomes, CSH Protoc. 2 (2008). pdb prot4903.

[77] T. Tumbar, G. Sudlow, A.S. Belmont, Large-scale chromatin unfolding and remodeling induced by VP16 acidic activation domain, J. Cell Biol. 145 (7) (1999) 1341–1354.

[78] M.S. Luijsterburg, M. Lindh, K. Acs, M.G. Vrouwe, A. Pines, H. van Attikum, L.H. Mullenders, N.P. Dantuma, DDB2 promotes chromatin decondensation at UV-induced DNA damage, J. Cell Biol. 197 (2) (2012) 267–281.

[79] I.F. Lau, S.R. Filipe, B. Soballe, O.A. Okstad, F.X. Barre, D.J. Sherratt, Spatial and temporal organization of replicating Escherichia coli chromosomes, Mol. Microbiol. 49 (3) (2003) 731–743.

[80] G. Urlaub, P.J. Mitchell, E. Kas, L.A. Chasin, V.L. Funanage, T.T. Myoda, J. Hamlin, Effect of gamma rays at the dihydrofolate reductase locus: deletions and inversions, Somat. Cell Mol. Genet. 12 (6) (1986) 555–566.

[81] J.S. Paige, K.Y. Wu, S.R. Jaffrey, RNA mimics of green fluorescent protein, Science 333 (6042) (2011) 642–646.

[82] A. Arora, M. Sunbul, A. Jaschke, Dual-colour imaging of RNAs using quencher- and fluorophore-binding aptamers, Nucleic Acids Res. (2015).

[83] S. Tyagi, Imaging intracellular RNA distribution and dynamics in living cells, Nat. Methods 6 (5) (2009) 331–338.

[84] L. Liang, D. Astruc, The copper(I)-catalyzed alkyne-azide cycloaddition (CuAAC) "click" reaction and its applications. An overview, Coord. Chem. Rev. 255 (23–24) (2011) 2933–2945.

[85] J.L. Goodier, P.K. Mandal, L. Zhang, H.H. Kazazian Jr., Discrete subcellular partitioning of human retrotransposon RNAs despite a common mechanism of genome insertion, Hum. Mol. Genet. 19 (9) (2010) 1712–1725.

[86] T. Chandra, K. Kirschner, J.Y. Thuret, B.D. Pope, T. Ryba, S. Newman, K. Ahmed, S.A. Samarajiwa, R. Salama, T. Carroll, R. Stark, R. Janky, M. Narita, L. Xue, A. Chicas, S. Nunez, R. Janknecht, Y. Hayashi-Takanaka, M.D. Wilson, A. Marshall, D.T. Odom, M.M. Babu, D.P. Bazett-Jones, S. Tavare, P.A. Edwards, S.W. Lowe, H. Kimura, D.M. Gilbert, M. Narita, Independence of repressive histone marks and chromatin compaction during senescent heterochromatic layer formation, Mol. Cell 47 (2) (2012) 203–214.

[87] P. Fraser, W. Bickmore, Nuclear organization of the genome and the potential for gene regulation, Nature 447 (7143) (2007) 413–417.

[88] P. Trojer, D. Reinberg, Facultative heterochromatin: is there a distinctive molecular signature?, Mol Cell 28 (1) (2007) 1–13.

[89] T. Cremer, M. Cremer, B. Hubner, H. Strickfaden, D. Smeets, J. Popken, M. Sterr, Y. Markaki, K. Rippe, C. Cremer, The 4D nucleome: Evidence for a dynamic nuclear landscape based on co-aligned active and inactive nuclear compartments, FEBS Lett. 589 (20 Pt A) (2015) 2931–2943.

[90] M. Furuno, K.C. Pang, N. Ninomiya, S. Fukuda, M.C. Frith, C. Bult, C. Kai, J. Kawai, P. Carninci, Y. Hayashizaki, J.S. Mattick, H. Suzuki, Clusters of internally primed transcripts reveal novel long noncoding RNAs, PLoS Genet. 2 (4) (2006) e37.

[91] T.R. Mercer, D. Wilhelm, M.E. Dinger, G. Solda, D.J. Korbie, E.A. Glazov, V. Truong, M. Schwenke, C. Simons, K.I. Matthaei, R. Saint, P. Koopman, J.S. Mattick, Expression of distinct RNAs from 3′ untranslated regions, Nucleic Acids Res. 39 (6) (2011) 2393–2403.

[92] F. Niazi, S. Valadkhan, Computational analysis of functional long noncoding RNAs reveals lack of peptide-coding capacity and parallels with 3′ UTRs, RNA 18 (4) (2012) 825–843.

[93] L.A. Boyer, K. Plath, J. Zeitlinger, T. Brambrink, L.A. Medeiros, T.I. Lee, S.S. Levine, M. Wernig, A. Tajonar, M.K. Ray, G.W. Bell, A.P. Otte, M. Vidal, D.K. Gifford, R.A. Young, R. Jaenisch, Polycomb complexes repress developmental regulators in murine embryonic stem cells, Nature 441 (7091) (2006) 349–353.

[94] A.P. Bracken, N. Dietrich, D. Pasini, K.H. Hansen, K. Helin, Genome-wide mapping of Polycomb target genes unravels their roles in cell fate transitions, Genes Dev. 20 (9) (2006) 1123–1136.

[95] A. Rego, P.B. Sinclair, W. Tao, I. Kireev, A.S. Belmont, The facultative heterochromatin of the inactive X chromosome has a distinctive condensed ultrastructure, J. Cell Sci. 121 (Pt 7) (2008) 1119–1127.

[96] C. Naughton, D. Sproul, C. Hamilton, N. Gilbert, Analysis of active and inactive X chromosome architecture reveals the independent organization of 30 nm and large-scale chromatin structures, Mol. Cell 40 (3) (2010) 397–409.

[97] R. Margueron, G. Li, K. Sarma, A. Blais, J. Zavadil, C.L. Woodcock, B.D. Dynlacht, D. Reinberg, Ezh1 and Ezh2 maintain repressive chromatin through different mechanisms, Mol. Cell 32 (4) (2008) 503–518.

[98] A. Kuzmichev, T. Jenuwein, P. Tempst, D. Reinberg, Different EZH2-containing complexes target methylation of histone H1 or nucleosomal histone H3, Mol. Cell 14 (2) (2004) 183–193.

[99] J. Zhao, T.K. Ohsumi, J.T. Kung, Y. Ogawa, D.J. Grau, K. Sarma, J.J. Song, R.E. Kingston, M. Borowsky, J.T. Lee, Genome-wide identification of polycomb-associated RNAs by RIP-seq, Mol. Cell 40 (6) (2010) 939–953.

[100] A. Kanhere, K. Viiri, C.C. Araujo, J. Rasaiyaah, R.D. Bouwman, W.A. Whyte, C.F. Pereira, E. Brookes, K. Walker, G.W. Bell, A. Pombo, A.G. Fisher, R.A. Young, R. G. Jenner, Short RNAs are transcribed from repressed polycomb target genes and interact with polycomb repressive complex-2, Mol. Cell 38 (5) (2010) 675–688.

[101] S. Kaneko, J. Son, S.S. Shen, D. Reinberg, R. Bonasio, PRC2 binds active promoters and contacts nascent RNAs in embryonic stem cells, Nat. Struct. Mol. Biol. 20 (11) (2013) 1258–1264.

[102] S. Kaneko, J. Son, R. Bonasio, S.S. Shen, D. Reinberg, Nascent RNA interaction keeps PRC2 activity poised and in check, Genes Dev. 28 (18) (2014) 1983–1988.

[103] S. Guil, M. Soler, A. Portela, J. Carrere, E. Fonalleras, A. Gomez, A. Villanueva, M. Esteller, Intronic RNAs mediate EZH2 regulation of epigenetic targets, Nat. Struct. Mol. Biol. 19 (7) (2012) 664–670.

[104] A.R. Karapetyan, C. Buiting, R.A. Kuiper, M.W. Coolen, Regulatory roles for long ncRNA and mRNA, Cancers (Basel) 5 (2) (2013) 462–490.

[105] R. Margueron, D. Reinberg, The Polycomb complex PRC2 and its mark in life, Nature 469 (7330) (2011) 343–349.

[106] N. Brockdorff, Noncoding RNA and Polycomb recruitment, RNA 19 (4) (2013) 429–442.

[107] C. Cifuentes-Rojas, A.J. Hernandez, K. Sarma, J.T. Lee, Regulatory interactions between RNA and polycomb repressive complex 2, Mol. Cell 55 (2) (2014) 171–185.

[108] I.F. Lau, S.R. Filipe, B. Søballe, O.-A. Økstad, F.-X. Barre, D.J. Sherratt, Spatial and temporal organization of replicating Escherichia coli chromosomes, Mol. Microbiol. 49 (3) (2003) 731–743.

[109] U. Schmidt, E. Basyuk, M.C. Robert, M. Yoshida, J.P. Villemin, D. Auboeuf, S. Aitken, E. Bertrand, Real-time imaging of cotranscriptional splicing reveals a kinetic model that reduces noise: implications for alternative splicing regulation, J. Cell Biol. 193 (5) (2011) 819–829.

[110] C.A. Schneider, W.S. Rasband, K.W. Eliceiri, NIH Image to ImageJ: 25 years of image analysis, Nat Methods 9 (7) (2012) 671–675.

[111] C. Davidovich, L. Zheng, K.J. Goodrich, T.R. Cech, Promiscuous RNA binding by Polycomb repressive complex 2, Nat. Struct. Mol. Biol. 20 (11) (2013) 1250–1257.

[112] J.G. Zalatan, M.E. Lee, R. Almeida, L.A. Gilbert, E.H. Whitehead, M. La Russa, J.C. Tsai, J.S. Weissman, J.E. Dueber, L.S. Qi, W.A. Lim, Engineering complex synthetic transcriptional programs with CRISPR RNA scaffolds, Cell 160 (1–2) (2015) 339–350.

[113] M.E. Tanenbaum, L.A. Gilbert, L.S. Qi, J.S. Weissman, R.D. Vale, A protein-tagging system for signal amplification in gene expression and fluorescence imaging, Cell 159 (3) (2014) 635–646.

[114] T. Jegou, Dynamics of Telomeres in a Telomerase Negative Human Osteosarcoma Cell, Ruprecht-Karls-Universität Heidelberg, Heidelberg, Faculty of Biosciences, 2007.

[115] M. Dundr, J.K. Ospina, M.H. Sung, S. John, M. Upender, T. Ried, G.L. Hager, A.G. Matera, Actin-dependent intranuclear repositioning of an active gene locus in vivo, J. Cell Biol. 179 (6) (2007) 1095–1103.